New physics search with flavour in the LHC era*

Tobias Hurth†
PRISMA Cluster of Excellence & Institute for Physics (THEP)
Johannes Gutenberg University, D-55099 Mainz, Germany

Farvah Mahmoudi‡
CERN Theory Division, Physics Department, CH-1211 Geneva 23, Switzerland
Clermont Université, Université Blaise Pascal, CNRS/IN2P3,
LPC, BP 10448, 63000 Clermont-Ferrand, France

We give a status report on quark flavour physics in view of the latest data from the B factories and the LHC, and discuss the impact of the latest experimental results on new physics in the MFV framework. We also show some examples of the implications in supersymmetry.

Contents

I. SM AND NEW PHYSICS FLAVOUR PROBLEMS

At the end of the B factories at SLAC (BaBar experiment) [1] and at KEK (Belle experiment) [2] and of the Tevatron B physics experiments [3, 4], all present measurements in flavour physics are consistent with the simple Cabibbo-Kobayashi-Maskawa (CKM) theory of the Standard Model (SM). The recent measurements by the high-statistics LHCb experiment [5] have not changed this feature. Of course there have been and there are still so-called tensions, anomalies, or puzzles in the quark flavour data at the 1-, 2-, or 3-σ level, however, until now they all have disappeared after some time when more statistics had been collected.

Thus, at least at present all flavour-violating processes between quarks are well-described by a 3×3 unitarity matrix, usually referred to as the CKM matrix [6, 7], which is fully described by four real parameters, three rotation angles and one complex phase. It is this complex phase that represents the only source of CP violation in the SM and that allows for a unified description of all the CP violating phenomena. This is an impressing success of the SM and the CKM theory.

It can be illustrated by the over-constrained triangles in the complex plane which reflect the unitarity of the CKM matrix, see Figure 1. Some historical CKM fits in Figure 2 illustrate the great success of the B factories. A closer look on the constraints is even more impressing: the constraints induced by CP conserving and by CP violating observables are fully consistent with each other (see Figure 3). Moreover, the tree-level observables which are in general assumed not being affected by new physics effects provide constraints which are fully consistent with the ones obtained from loop-induced observables (see Figure 4). Especially this feature has been somehow unexpected because in principle (loop-induced) flavour changing neutral current (FCNC) processes like $\bar{B} \to X_s\gamma$ offer high sensitivity to new physics (NP) due

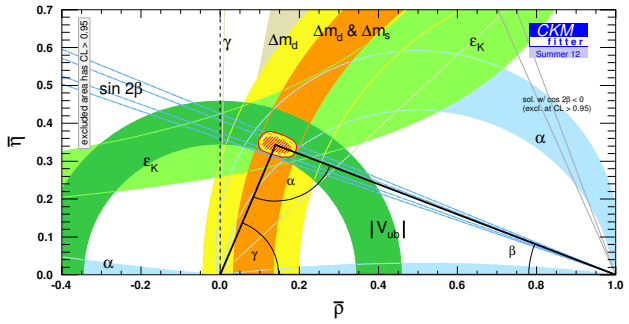

FIG. 1: Constraints in the $(\bar{\rho},\bar{\eta})$ plane. The red hashed region of the global combination corresponds to 68% C.L. [8]

*Based on invited plenary talks given by T.H. at PASCOS2012, the 18th International Symposium on Particles, Strings and Cosmology, Merida, Mexico, 3rd-8th of June 2012, and at the Third Workshop on the Implications of LHC Results for TeV-scale Physics, CERN, Geneva, 13th-17th of July 2012.

†Electronic address: tobias.hurth@cern.ch
‡Electronic address: mahmoudi@in2p3.fr

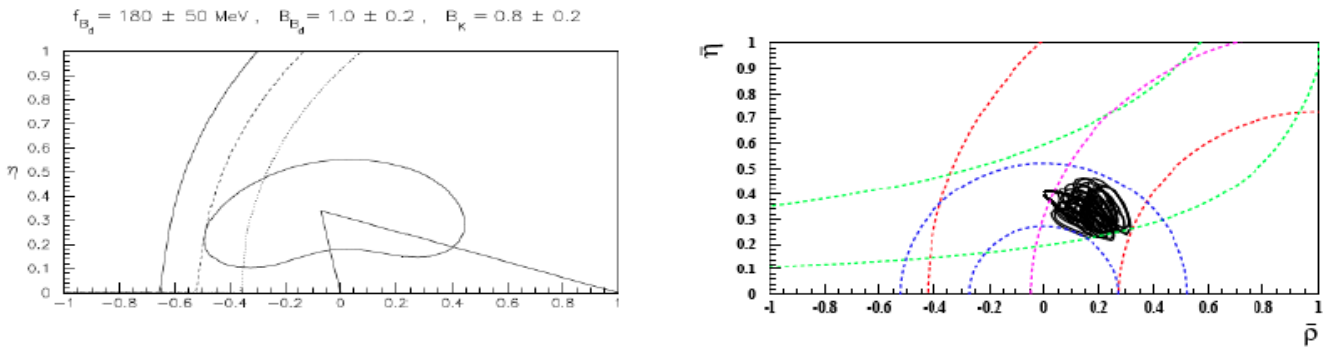

FIG. 2: Some historical CKM fits of Ali and London, 1995 (left), of Plazczynski and Schune, 1999 (right).

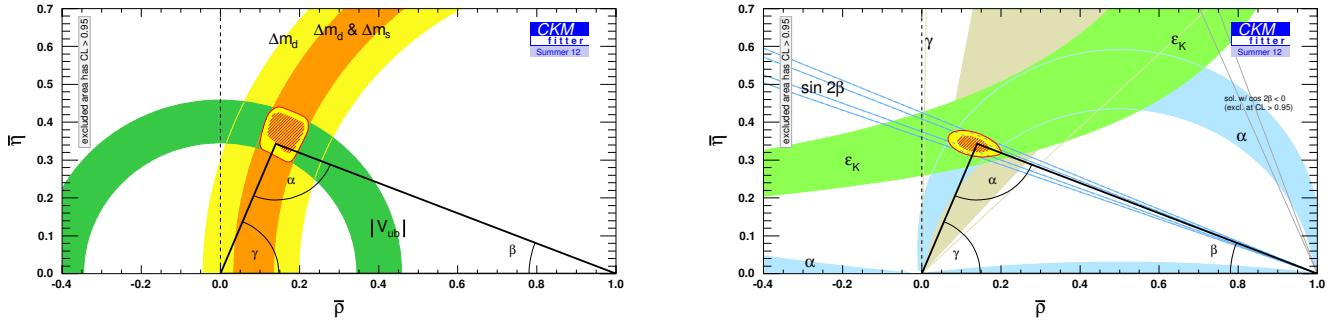

FIG. 3: Constraints from CP conserving (left) and CP violating (right) quantities only [8].

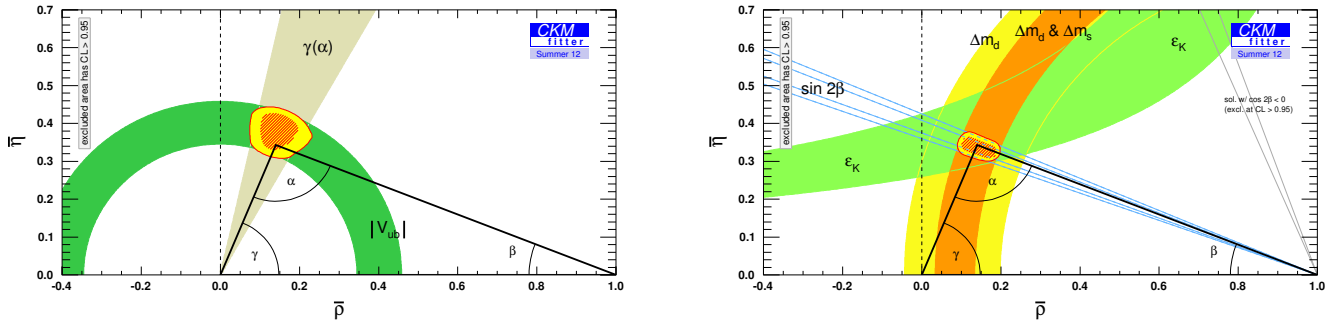

FIG. 4: Constraints from "Tree" (left) and "Loop" (right) quantities only [8].

to the simple fact that additional contributions to the decay rate, in which SM particles are replaced by new particles such as the supersymmetric charginos or gluinos, are not suppressed by the loop factor $\alpha/4\pi$ relative to the SM contribution, see Figure 5.

It is worth mentioning that there is much more flavour data not shown in the unitarity fits which confirms the SM predictions of flavour mixing like rare decays. This success of the CKM theory was honoured by the Nobel Prize in physics in 2008.

The absence of any unambiguous sign for NP in the flavour data but *also* in the high-p_T data of the ATLAS and CMS experiments [9, 10] guides our attention to the well-known flavour problem of NP: in the model-independent approach using the effective electroweak Hamiltonian, the contribution to one specific operator $\mathcal{O}_i$ can be parametrised via $(C^i_{\rm SM}\,/\,M_W + C^i_{\rm NP}\,/\,\Lambda_{\rm NP}) \times \mathcal{O}_i$ where the first term represents the SM contribution at the electroweak scale M_W and the second one the NP contribution with an unknown coupling $C^i_{\rm NP}$ and an unknown NP scale $\Lambda_{\rm NP}$. The non-existence of large NP effects in FCNC observables in general asks for an explanation why FCNC are suppressed. This famous flavour problem of NP can be solved in two ways: either the mass scale of the new degrees of freedom $\Lambda_{\rm NP}$ is very high or the new flavour-violating couplings $C^i_{\rm NP}$ are small for (symmetry?) reasons that remain to be found. For example, assuming *generic* new flavour-violating couplings of $O(1)$, the present data on K-$\bar{K}$ mixing implies a very high NP scale of order 10^3–10^4 TeV depending on whether the

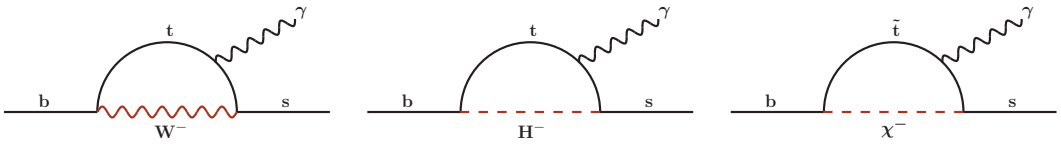

FIG. 5: Loop-induced $\bar{B} \to X_s\gamma$ decay via the SM particles, W^- boson and top quark t (left), via new particle, namely charged Higgs H^- and top quark t (middle), or via new supersymmetric particles, chargino $\tilde{\chi^-}$ and stop $\tilde{t}$ (right) .

new contributions enter at loop- or at tree-level. In contrast, theoretical considerations on scale hierarchies in the Higgs sector, which is responsible for the mass generation of the fundamental particles in the SM, call for NP at order 1 TeV. But any NP below the 1 TeV scale must have a non-generic flavour structure.

These considerations also imply that FCNC decays provide information about the SM and its extensions via virtual effects to scales presently not accessible by the direct search for new particles (for reviews see Refs. [11, 12]). Thus, the information offered by the FCNC is complementary to the one provided by the high-p_T experiments ATLAS and CMS [13, 14]. It is also obvious, that the indirect information on NP by FCNC (even if SM-like) will be most valuable when the general nature of NP will be identified in the direct search, especially when the mass scale of NP will be fixed.

Indeed, in the SM the Glashow-Iliopoulos-Maiani (GIM) mechanism, small CKM elements and often helicity, all suppress FCNC processes. These suppression factors stem from the particle content of the SM and the unexplained smallness of most Yukawa couplings and are absent in generic extensions of the SM. Hence FCNCs are an excellent testing ground to probe new physics up to scales of 100 TeV, depending on the model. Moreover, CP violation in flavour-changing transitions of the SM is governed by a single parameter, the phase of the CKM matrix, so that the SM is highly predictive about CP physics. Certain CP asymmetries are practically free of hadronic uncertainties, which permits the extraction of fundamental CP phases from experiments with high accuracy. Thus, CP physics is a powerful tool to probe extensions of the SM, which generically involve many new CP phases.

As a consequence, the present data of the B physics experiments already imply significant restrictions for the parameter space of new physics models – as we will explicitly show below – and lead to important clues for the direct search for new particles and for model building beyond the SM.

Thus, the CKM mechanism is the dominating effect for CP violation and flavour mixing in the quark sector; however, there is still room for sizeable new effects and new flavour structures because the flavour sector has only been tested at the 10% level especially in the $b-s$ sector. Moreover, the Standard Model does not describe the flavour phenomena in the lepton sector due to the existence of neutrino masses, a property not described by the SM.

Furthermore, while the gauge principle governs the gauge sector of the SM there is no guiding principle in the flavour sector: the CKM mechanism (three Yukawa SM couplings) provides a phenomenological description of quark flavour processes, but leaves the significant hierarchy of the quark masses and the mixing parameters – observed in experiment – unexplained. This problem is often referred to as the flavour problem of the SM.

The Randall-Sundrum model is a popular approach to this SM flavour problem. The hierarchy of the flavour parameters can be explained by the special geometrical settings of the model. In addition the so-called gauge-hierarchy problem in the Higgs sector finds a natural explanation in this model [15–17].

The SM flavour problem is also reflected in the fact that many open fundamental questions of particle physics are related to flavour:

- How many families of fundamental fermions are there?
- How are neutrino and quark masses and mixing angles generated?
- Do there exist new sources of flavour and CP violation?
- Is there CP violation in the QCD gauge sector?
- Are there relations between the flavour structure in the lepton and quark sectors?

There is already experimental evidence beyond the SM which is partially connected to flavour physics: the existence of dark matter, the non-zero neutrino masses, and the baryon asymmetry of the universe; the latter implies the need for new sources of CP violation beyond the one offered by the SM. This provides an important link between particle physics and cosmology.

In the following sections, we discuss the latest key measurements by LHCb, the B factories, and the Tevatron experiments.

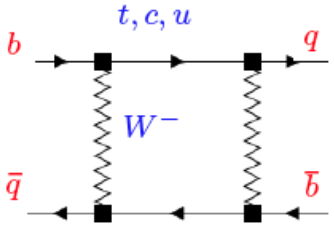

FIG. 6: $B_q - \bar{B}_q$ mixing governed by the box diagram.

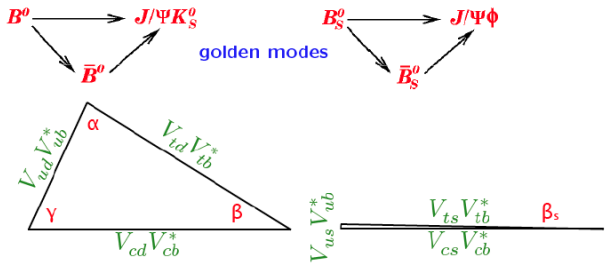

FIG. 7: CP violating through interference of decay with and without mixing in the two golden modes of the B_d and B_s system.

II. LATEST MEASUREMENTS AT HADRON COLLIDERS

A. New physics in $B_q - \bar{B}_q$ mixing (q=d,s)?

The meson-antimeson oscillation is governed by two parameters, the mass difference (ΔM) of the two physical eigen states B_H and B_L and the decay rate difference ($\Delta\Gamma$):

$$\Delta M := M_H - M_L = 2|M_{12}|\,, \quad (1)$$
$$\Delta\Gamma := \Gamma_L - \Gamma_H = 2|\Gamma_{12}|\cos\Phi\,. \quad (2)$$

$|M_{12}|$ corresponds to the dispersive part of the box diagram in Figure 6 which is sensitive to new heavy particles while Γ_{12} corresponds to its absorptive part which is sensitive to the light internal particles, and, thus, often assumed to be insensitive to NP. Possible NP effects can be parametrised by the complex parameter Δ_q ($q = d, s$): $M_{12,q} = M_{12,q}^{SM} \times \Delta_q$ in a model-independent way. There are several observables which are sensitive to the NP phase $arg(\Delta_q) = \Phi_q^\Delta$, for example ΔM_q and $\Delta|\Gamma_q| = 2|\Gamma_{12,q}| \times \cos(\Phi_q^{SM} + \Phi_q^\Delta)$. But also the golden modes $B_d \to J/\psi K_s^0$ and $B_s \to J/\psi\Phi$ are sensitive to the NP phases. The corresponding CP violating phases in the SM β_q^{SM} are modified via $2\beta_d^{SM} + \Phi_d^\Delta$ and $2\beta_s^{SM} - \Phi_s^\Delta$.

As illustrated in Figure 7, the CP violating phase in $B_s \to J/\psi\Phi$ is very small in the SM [18]:

$$2\beta_s^{SM} = -\arg\left((V_{ts}V_{tb}^*)^2/(V_{cs}V_{cb}^*)^2\right) = (2.1 \pm 0.1)^0. \quad (3)$$

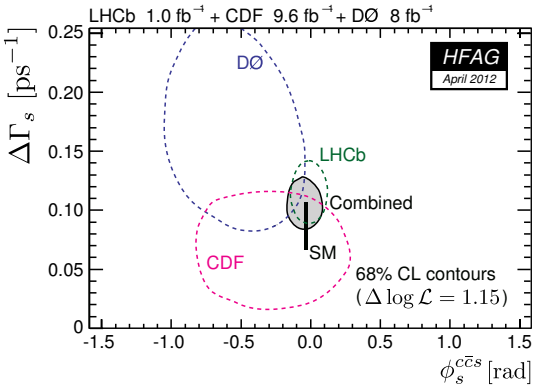

FIG. 8: HFAG 2012 combination of ϕ_s and $\Delta\Gamma_s$ results [59].

LHCb has reported a measurement of this small angle [19] which is fully consistent with the SM prediction and also consistent with the previous measurements of CDF and D0. In addition, LHCb has resolved the two-fold ambiguity [20] and reported their first measurement of $\Delta\Gamma_s$ which confirms the Heavy Quark Expansion prediction:

$$\Delta\Gamma_s(\text{LHCb}) = (0.116 \pm 0.019)\ \text{ps}^{-1}, \quad [19] \quad (4)$$
$$\Delta\Gamma_s(\text{HFAG}) = (0.105 \pm 0.015)\ \text{ps}^{-1}, \quad [59] \quad (5)$$
$$\Delta\Gamma_s(\text{SM}) = (0.087 \pm 0.021)\ \text{ps}^{-1}, \quad [21] \quad (6)$$

and

$$\phi_s(\text{LHCb}) = (-0.001 \pm 0.104)\ \text{rad}, \quad [19] \quad (7)$$
$$\phi_s(\text{HFAG}) = (-0.044^{+0.090}_{-0.085})\ \text{rad}, \quad [59] \quad (8)$$
$$\phi_s(\text{SM}) = (-0.036 \pm 0.002)\ \text{rad}. \quad [21] \quad (9)$$

Thus, NP contributions in the mixing of the B_s system are disfavoured by the present data (see Figure 8).

Furthermore, the semi-leptonic asymmetries offer an independent test of NP physics in $B_q - \bar{B}_q$ mixing. In the presence of NP they get modified via

$$a_{sl}^q = \text{Im}\left(\frac{\Gamma_{12,q}}{M_{12,q}}\right) = \left(\frac{|\Gamma_{12,q}|}{|M_{12,q}|}\right)\frac{\sin(\Phi_q^{SM} + \Phi_q^\Delta)}{|\Delta_q|}. \quad (10)$$

D0 had measured the dimuon charge asymmetry to disagree with the SM prediction by 3.9σ [21, 22]:

$$A_{sl}^b(\text{D0}) = -(7.87 \pm 1.72 \pm 0.93) \times 10^{-3}, \quad (11)$$
$$A_{sl}^b(\text{SM}) = -(0.28^{+0.05}_{-0.06}) \times 10^{-3}, \quad (12)$$

where A_{sl}^b is a linear combination of the semi-leptonic asymmetries a_{sl}^d and a_{sl}^s. As was argued in Ref. [23] , the central value of the D0 measurement is larger than theoretically possible. More recently, there are also direct measurements of a_{sl}^s and a_{sl}^d by D0 [24] which in combination with the dimuon charge asymmetry still leads to a 3σ deviation from the SM prediction, see left plot of Figure 9. In contrast, the first LHCb measurement

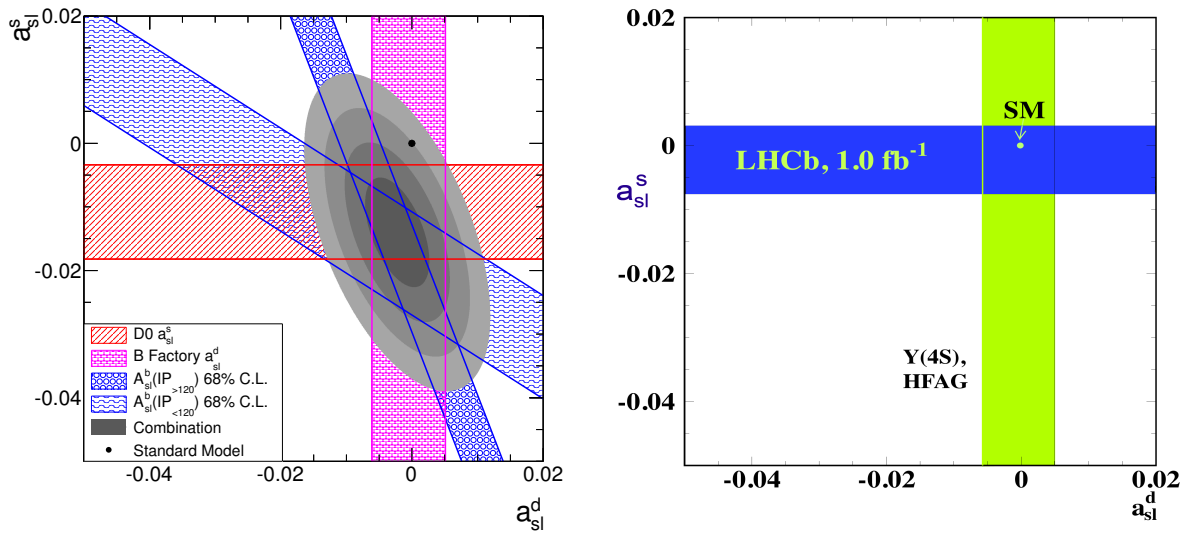

FIG. 9: Measurements of the semileptonic CP asymmetries a^d_{sl} and a^s_{sl} by D0 (left) and by LHCb and B factories (right).

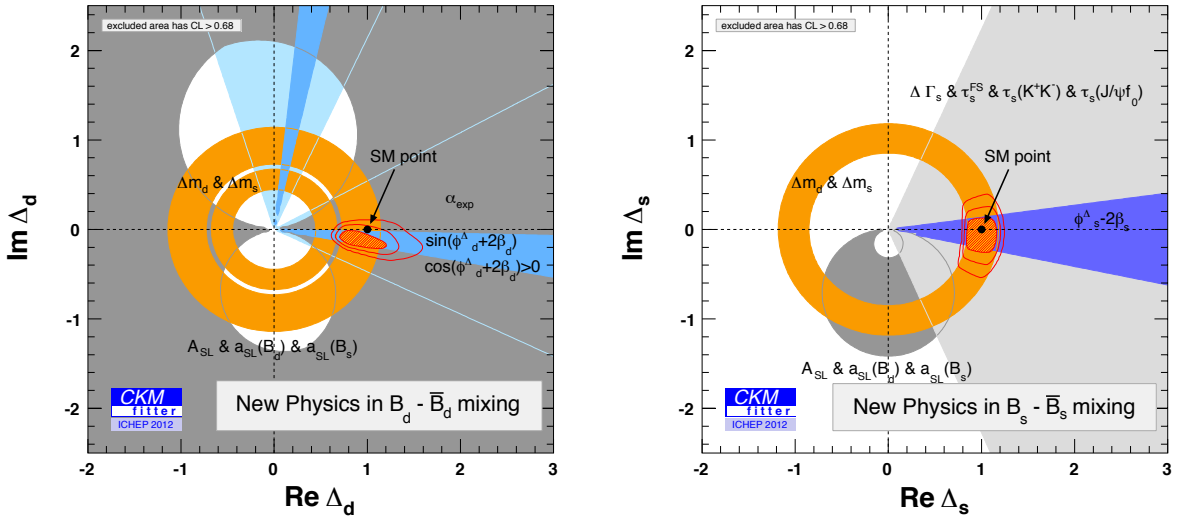

FIG. 10: New physics in $B_d - \bar{B}_d$ (left) and in $B_s - \bar{B}_s$ (right) mixing: fit result for the complex parameters Δ_d and Δ_s, respectively. The red area shows the region with C.L. $< 68.3\%$ while the two additional contour lines inscribe the regions with C.L. $< 95.45\%$ and C.L. $< 99.73\%$, respectively [8].

of a^s_{sl} [25] and the measurement of a^d_{sl} by the B factories [59] are nicely compatible with the SM predictions, see right plot of Figure 9. Obviously, there is a slight tension between the two data sets which calls for improved measurements.

Finally, we mention that within the model-independent analysis of NP in $B_d - \bar{B}_d$ mixing, a 1.6σ deviation is obtained for the 2-dimensional SM hypothesis $\Delta_d = 1$. Figure 10 shows the fit result for the complex parameter Δ_d. It is worth mentioning that a NP phase $\Phi^{\Delta}_d < 0$ would resolve the slight tension between BR$(B \to \tau\nu)$ and $\sin\beta$ in the global CKM fit (see subsection III B). We also state that in the B_s system the CKMfitter group finds a 0.2σ deviation for the corresponding SM hypothesis $\Delta_s = 1$, see Figure 10. A detailed discussion can be found in [26].

B. Angular observables in $B \to K^*\ell^+\ell^-$

The semi-leptonic decay $B \to K^*\ell^+\ell^-$ is mediated by electroweak loop diagrams in the SM and can receive large enhancements from NP. It gives access to a vari-

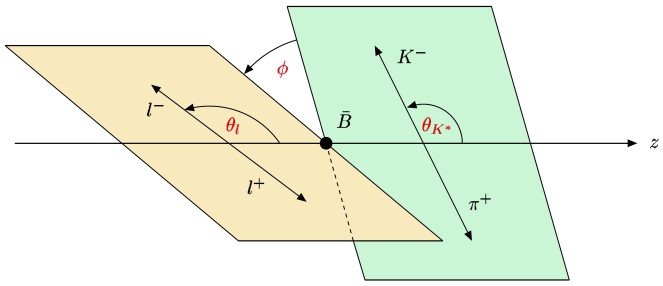

FIG. 11: Kinematic variables in $B \to K^* \ell^+ \ell^-$.

ety of angular observables and hence offers a rich phenomenology. From the theoretical point of view, exclusive modes suffer from large hadronic uncertainties due to the form factors. One has to find strategies to reduce this form factor dependence by considering appropriate ratios. On the contrary, the experimental measurements are easier here as compared to the case of inclusive modes.

Two kinematic regimes are considered in order to avoid the narrow $c\bar{c}$ resonances. In the region where the dimuon invariant mass squared, q^2, is small ($1 < q^2 < 6$ GeV^2) the decay is described by the QCD-improved Factorisation (QCDF) and the Soft-Collinear Effective Theory (SCET). In the high q^2 region ($q^2 \gtrsim 14$ GeV^2) on the other hand the Operator Product Expansion (OPE) is used. As the theoretical treatments in the low- and high-q^2 regions are based on different theoretical concepts, the consistency of the consequences from the two regimes allows for important cross checks.

The angular distribution of $B \to K^* \ell^+ \ell^-$ with $K^* \to K^+ \pi^-$ can be fully described in terms of four kinematic variables, the angles $\theta_\ell, \theta_K, \phi$ and q^2 as shown in Figure 11. There are twelve angular terms appearing in the differential decay rate that can be exploited experimentally. The full expressions for these functions can be found in [27, 28].

Several angular observables, namely the differential branching ratio, forward-backward asymmetry (A_{FB}) and K^* longitudinal fraction (F_L), have already been measured by the Belle and BaBar experiments, and also CDF and LHCb. In addition, LHCb has also measured S_3 which is related to the asymmetry between the K^* parallel and perpendicular spin amplitudes, and the value of q_0^2 for which the differential forward-backward asymmetry vanishes. The experimental results as well as the SM predictions for these observables are summarised in Table I. They agree within the current errors.

In the Constrained MSSM (CMSSM), A_{FB} and q_0^2 are particularly constraining. The CMSSM is governed by only five additional universal parameters defined at the $M_{\rm GUT}$ scale: the mass of the scalar particles, m_0, the mass of the gauginos, $m_{1/2}$, the trilinear coupling, A_0, the ratio of the vacuum expectation values of the Higgs doublet, $\tan\beta$, and finally the sign of the higgsino mass term, μ. In Figure 12 the SUSY spread is compared to the LHCb 1 and 2σ bounds in the CMSSM parameter space with $\tan\beta = 50$ and $A_0 = 0$ [29].

With 2–3 fb^{-1} of integrated luminosity, LHCb will have the opportunity of performing a full angular analysis. This calls in turn for optimised set of observables with reduced theoretical uncertainty. In particular, as the amplitudes depend linearly on the soft form factors at leading order in the low-q^2 region, a complete cancellation of the hadronic uncertainties could be possible in leading order, which consequently increases the sensitivity to new physics. In the high-q^2 region, there are improved Isgur-Wise relations between the form factors which allow to construct optimal observables.

Examples of such observables are the transversity amplitudes, $A_T^{(2,3,4,5)}$ [27, 28] (or similarly $P_{1\ldots6}$ [30] and $H_T^{(1,2,3)}$ [31]). The sensitivity of $A_T^{(2)}$ to NP scenarios is illustrated in Figure 13. There exist a large number of analyses on the NP sensitivity showing the rich phenomenology of the angular observables [27–35].

C. Implications of the latest measurements of $B_s \to \mu\mu$

The rare decay $B_s \to \mu^+\mu^-$ proceeds via Z^0 penguin and box diagrams in the SM, see Figure 14. It is highly helicity-suppressed by a suppression factor m_μ/m_b on the amplitude level. As a consequence the SM prediction for the branching ratio of the decay $B_s \to \mu^+\mu^-$ is of order 10^{-9}. However, the branching ratio can be much larger within specific extensions of the SM. For example, the helicity-suppression of the SM contribution leads to an enhanced sensitivity to the Higgs-mediated scalar FCNCs within the 2HDM and, especially within the MSSM, see Figure 14. These non-standard contributions lead to a drastic enhancement in the large $\tan\beta$-limit [36–38]. In the MSSM there is an enhancement factor of $(\tan\beta)^3$ on the amplitude level. The best upper limit for $\mathrm{BR}(B_s \to \mu^+\mu^-)$ measured in a single experiment comes from LHCb [39]:

$$\mathrm{BR}(B_s \to \mu^+\mu^-) < 4.5 \times 10^{-9} \qquad (13)$$

at 95% C.L. This upper limit is followed by the result from CMS, $\mathrm{BR}(B_s \to \mu^+\mu^-) < 7.7 \times 10^{-9}$ [40]. The CDF collaboration obtains a 95% C.L. upper limit, $\mathrm{BR}(B_s \to \mu^+\mu^-) < 3.4 \times 10^{-8}$ [41], together with a one sigma interval, $\mathrm{BR}(B_s \to \mu^+\mu^-) = (1.3^{+0.9}_{-0.7}) \times 10^{-8}$, coming from an observed excess over the expected background. The ATLAS collaboration has announced the upper limit, $\mathrm{BR}(B_s \to \mu^+\mu^-) < 2.2 \times 10^{-8}$ [42]. The combination of LHCb, ATLAS and CMS results leads to an upper bound of 4.2×10^{-9} [43].

Very recently, the LHCb collaboration announced the first evidence for the decay $\mathrm{BR}(B_s \to \mu^+\mu^-)$ with the branching ratio [44]:

$$\mathrm{BR}(B_s \to \mu^+\mu^-) = \left(3.2^{+1.4}_{-1.2}(\mathrm{stat})^{+0.5}_{-0.3}(\mathrm{syst})\right) \times 10^{-9}. \qquad (14)$$

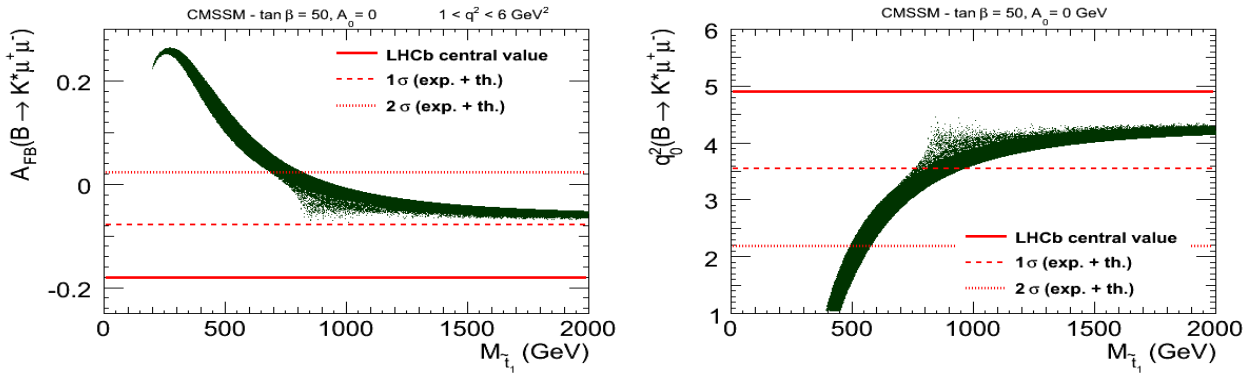

FIG. 12: SUSY spread of A_{FB} (left) and the A_{FB} zero-crossing, q_0^2 (right) as a function of the lightest stop mass in the CMSSM for $\tan\beta = 50$ and $A_0 = 0$.

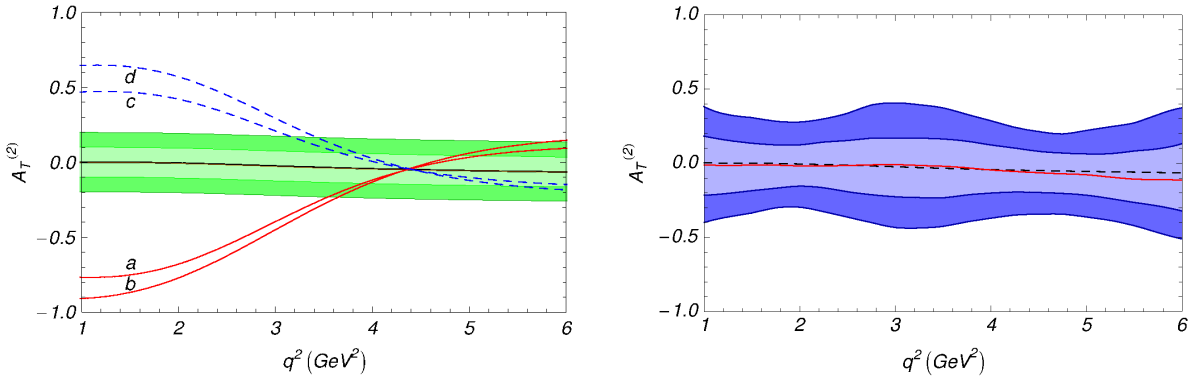

FIG. 13: The theoretical errors (left) for $A_T^{(2)}$ are compared to the experimental errors (right) as a function of q^2. Light green bands include an estimated Λ/m_b uncertainty at a $\pm 5\%$ level and the dark green bands correspond to a $\pm 10\%$ correction. The curves labelled (a)–(d) correspond to different benchmark SUSY scenarios [27]. In the right plot, the light and dark blue bands correspond to 1σ and 2σ statistical errors with a yield corresponding to 10 fb^{-1} data from LHCb, respectively.

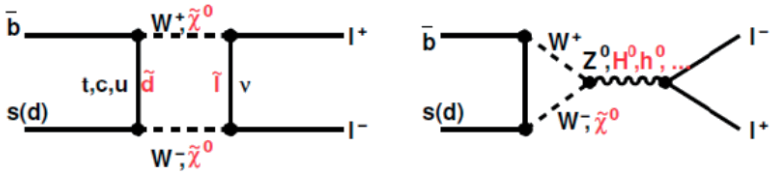

FIG. 14: Contributions to the rare decay $B_s \to \mu^+\mu^-$ in the SM (black) and in the MSSM (red).

This new measurement is a major step which will hopefully be followed by more precise results. The present accuracy however does not lead to improved constraints on supersymmetry as compared to the one from the previous upper limit. Nevertheless, as we will see later, the lower bound has consequences on the constraints on the Wilson coefficients in the MFV framework.

All these results are very close to the SM prediction, which is $\mathrm{BR}(B_s \to \mu^+\mu^-) = (3.53 \pm 0.38) \times 10^{-9}$ [29]. The main theoretical uncertainty comes from the B_s decay constant, which is now in the focus of the lattice gauge theory community, see Refs. [45–50].

The theoretical prediction does not directly correspond to the experimental branching ratio. There are two correction factors of $O(10\%)$: one includes the effect of the $\bar{B}_s - B_s$ oscillation [51, 52], the other takes into account effects of soft radiation [53].

In an exemplary mode we show the strong restriction power of this data on the parameter space of the CMSSM as presented in Refs. [13, 54]. In Figure 15, taken from Ref. [13], constraints from flavour observables on the CMSSM in the plane $(m_{1/2}, m_0)$ for $\tan\beta = 50$ and $A_0 = 0$, are shown, in the left with the 2011 results for $\mathrm{BR}(B_s \to \mu^+\mu^-)$, and in the right with the 2012

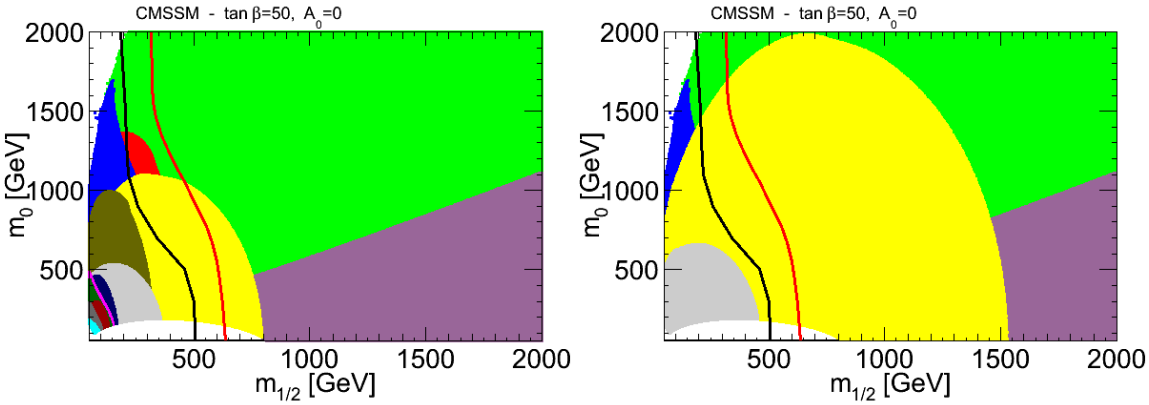

FIG. 15: Constraints from flavour observables on the CMSSM in the plane $(m_{1/2}, m_0)$ for $\tan\beta = 50$ with 2010 results on $\mathrm{BR}(B_s \to \mu^+\mu^-)$ (left) and with the 2011 results (right).

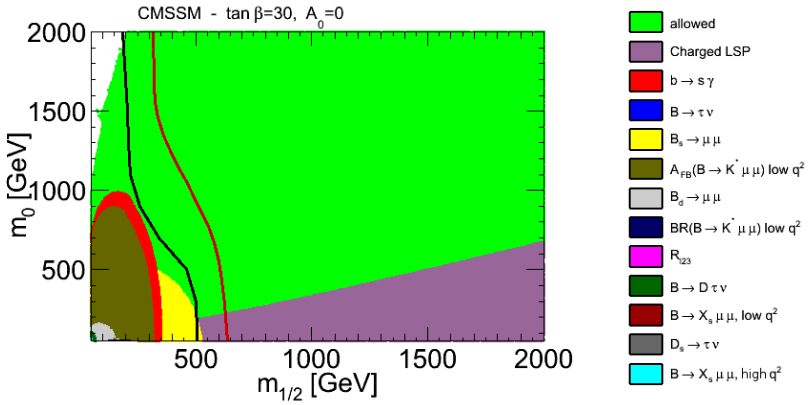

FIG. 16: Constraints from flavour observables in CMSSM in the plane $(m_{1/2}, m_0)$ for $\tan\beta = 30$.

Moriond results. The colour code is as in Figure 16. The black line corresponds to the CMS SUSY exclusion limit with 1.1 fb^{-1} of data [55] and the red line to the CMS SUSY exclusion limit with 4.4 fb^{-1} of data [56] at 7 TeV. One notice that while with more integrated luminosity the direct limit is slightly shifted to higher masses, the constraining power of the new $\mathrm{BR}(B_s \to \mu^+\mu^-)$ limit has impressively increased and overpassed the direct limit for high values of $\tan\beta$.

Figure 16 shows that the rare decay $\mathrm{BR}(B_s \to \mu^+\mu^-)$ is mainly sensitive for the large $\tan\beta$ region.

III. LATEST NEWS FROM THE B FACTORIES

A. News on inclusive penguins?

The inclusive decay $\bar{B} \to X_s\gamma$ is a good example to confirm the simple CKM theory of flavour mixing in the SM, not shown in the CKM unitarity fit. While non-perturbative corrections to this decay mode are subleading and recently estimated to be well below 10% [57], perturbative QCD corrections are the most important corrections. Within a global effort, a perturbative QCD calculation to the next-to-next-to-leading-logarithmic order level (NNLL) has been performed and has led to the first NNLL prediction of the $\bar{B} \to X_s\gamma$ branching fraction [58] with a photon cut at $E_\gamma = 1.6$ GeV (including the error due to nonperturbative corrections):

$$\mathrm{BR}(\bar{B} \to X_s\gamma)_{\mathrm{NNLL}} = (3.15 \pm 0.23) \times 10^{-4}. \qquad (15)$$

Using updated input parameters from PDG in particular for the quark masses and the CKM elements, the central value is shifted to 3.08×10^{-4}. The combined experimental data by HFAG leads to [59]

$$\mathrm{BR}(\bar{B} \to X_s\gamma) = (3.43 \pm 0.21 \pm 0.07) \times 10^{-4}, \qquad (16)$$

where the first error is combined statistical and systematic, and the second is due to the extrapolation in the photon energy. Thus, the SM prediction and the experimental average are consistent at the 1.2σ level. As a consequence, the $\bar{B} \to X_s\gamma$ has very restrictive power on

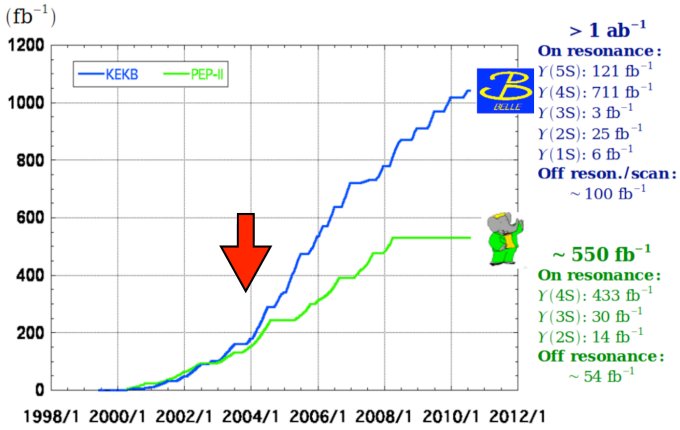

FIG. 17: Integrated luminosity of the B factories.

the parameter space of NP models. Recently, the first practically complete NLL calculation of this decay in the MSSM has been finalised [60, 61].

The inclusive semi-leptonic decay $B \to X_s \ell^+ \ell^-$ could in principle play a similar role in the NP search. The NNLL QCD calculation has been finalised some time ago and even electromagnetic corrections have been calculated recently. The theoretical accuracy is of order of 10% [62]. However, unfortunately the *latest* measurements of this inclusive decay mode of the B factories stem from 2004 in case of BaBar based on $89 \times 10^6 B\bar{B}$ events [63] and from 2005 in case of Belle based on $152 \times 10^6 B\bar{B}$ events [64]. As the graph of the integrated luminosity (Figure 17) shows these numbers of events correspond to less than 30% of the data set available at the end of the B factories. It would be highly desirable that new analyses are worked out which are based on the complete data sets. For further details on inclusive penguin decays we refer the reader to the recent mini-review on penguins [65].

B. New physics in $B \to \tau\nu$?

For some time there has been a tension between the direct measurement and the indirect fit of the branching ratio $\mathrm{BR}(B \to \tau\nu)$ at the 2.8σ level. Moreover, as was pointed out by the CKMfitter group [8], there has been a specific correlation between $\sin\beta$ and $\mathrm{BR}(B \to \tau\nu)$ which is also a bit at odds, see Figure 18. Obviously the measured value of $\sin\beta$ has been too low, while the one of $\mathrm{BR}(B \to \tau\nu)$ has been too large. Interestingly, this tension could have been solved by a negative NP mixing phase in the B_d system, $\Phi_d^\Delta < 0$.

In principle, one could think that this tension could also be solved by a NP contribution to $\mathrm{BR}(B \to \tau\nu)$ induced by a charged Higgs in the popular Two-Higgs Doublet model of Type II, see left diagram in Figure 19. In the later model the SM branching ratio gets modified in the following way:

$$\mathrm{BR}(B \to \tau\nu) = \mathrm{BR}_{SM} \times \left(1 - \frac{m_B^2}{m_{H^+}^2} \tan^2\beta\right)^2 \qquad (17)$$

But for the allowed values of the ratio of the quantity $\tan\beta$ and the charged Higgs mass m_{H^+} due to constraints by other flavour data one only gets a reduction compared to the SM branching ratio.

However, Belle has recently presented a new measurement with new data and an improved analysis method including also a reanalysis of the old data which shows a significant lower value in good agreement with the global fit, while the new Babar measurement confirms the old high value. The various measurements are shown in Figure 20. As a result the indirect fit prediction for $\mathrm{BR}(B \to \tau\nu)$ and direct measurements presently deviate by 1.6σ only, see Figure 18.

More recently a similar tension has showed up in $B \to D\tau\nu$ and $B \to D^*\tau\nu$. Based on its full data sample, Babar has reported an improved measurements of the specific ratios [66]:

$$\begin{aligned} \mathcal{R}_{\tau/\ell} &= \mathrm{BR}(B \to D\tau\nu)/\mathrm{BR}(B \to D\ell\nu) \qquad (18) \\ &= 0.440 \pm 0.058 \pm 0.018 \\ \mathcal{R}^*_{\tau/\ell} &= \mathrm{BR}(B \to D^*\tau\nu)/\mathrm{BR}(B \to D^*\ell\nu) \qquad (19) \\ &= 0.332 \pm 0.024 \pm 0.018. \end{aligned}$$

They exceed the SM expectations by 2.0σ and 2.7σ, respectively [67–69].

These ratios are rather sensitive to new physics contributions because the hadronic form factors tend to cancel. For example, they are sensitive to the charged Higgs, see right diagram in Figure 19. But again the THDM-II does not offer a consistent explanation of the two ratios; for the allowed values of $\tan\beta/m_{H^+}$, one finds an explanation for $\mathcal{R}$ but not for $\mathcal{R}^*$. As shown in Ref. [70], a consistent explanation of both ratios is possible in the THDM of type III. Interestingly, the authors of Ref. [71] argue that MFV (see next section) is disfavoured as explanation of this anomaly and spot various models with general flavour structures for it. Since the current result still suffers from large systematic uncertainty due to the background, the updated BaBar results and confirmation from Belle are awaited to clarify the situation.

IV. MFV BENCHMARK

At this stage of the NP search using rare B and kaon decays, it makes sense to analyse the impact of the measurements within the framework of minimal flavour violation (MFV). The hypothesis of MFV [72–75], is a formal model-independent solution to the NP flavour problem. It assumes that the flavour and the CP symmetries are broken as in the SM. Thus, it requires that all flavour- and CP-violating interactions be linked to the known structure of Yukawa couplings. A renormalisation-group

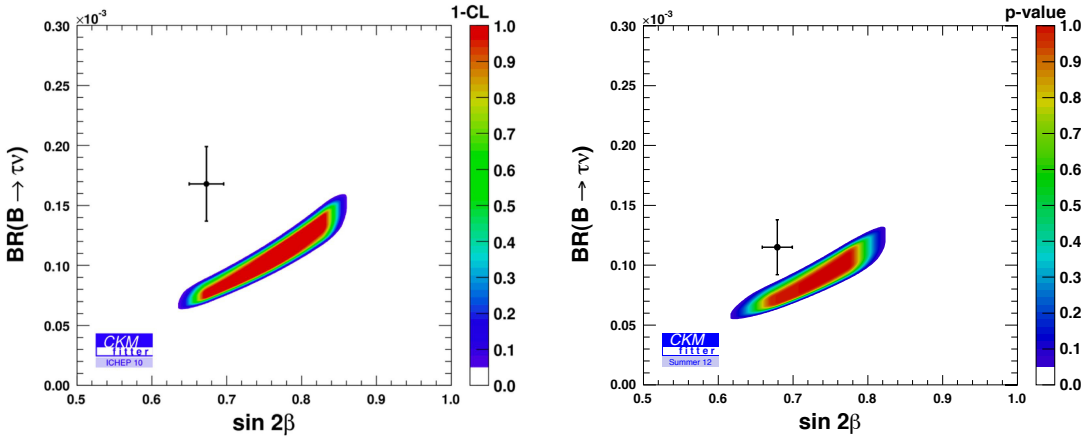

FIG. 18: Correlation of BR($B \to \tau\nu$) and $\sin\beta$ based on Pre-ICHEP12 data (left) and on ICHEP12 data (right); cross corresponds to the experimental values with 1σ uncertainties [8].

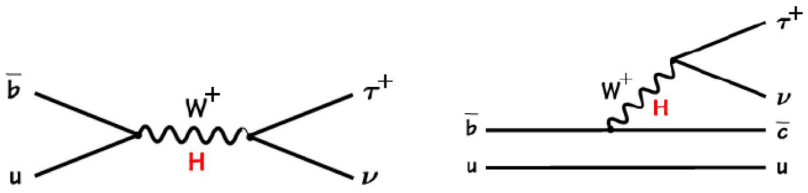

FIG. 19: Tree contributions to BR($B \to \tau\nu$) (left) and to BR($B \to D\tau\nu$) (right).

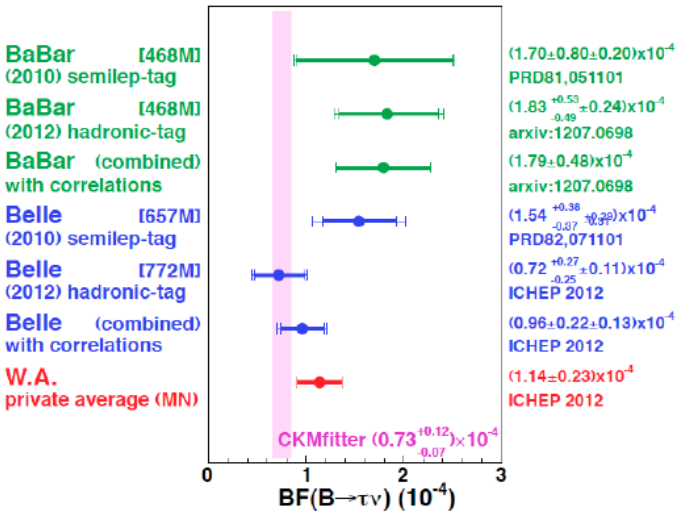

FIG. 20: ICHEP12 data: various measurements of BR($B \to \tau\nu$) with the new world average, courtesy of M. Nakao.

invariant definition of MFV based on a symmetry principle is given in Ref. [74]; this is mandatory for a consistent effective field theoretical analysis of NP effects (for a recent mini-review see Ref. [76]).

The MFV hypothesis represents an important benchmark in the sense that any measurement which is inconsistent with the general constraints and relations induced by the MFV hypothesis unambiguously indicates the existence of new flavour structures. Moreover, compared with a general model-independent analysis as presented in Ref. [35, 77, 78], the number of free parameters is heavily reduced due to the additional MFV relations. Indeed there are two strict predictions in this general class of models which have to be tested. First, the MFV hypothesis implies the usual CKM relations between $b \to s$, $b \to d$, and $s \to d$ transitions. For example, this relation allows for upper bounds on NP effects in BR($\bar{B} \to X_d\gamma$), and BR($\bar{B} \to X_s\nu\bar{\nu}$) using experimental data or bounds from BR($\bar{B} \to X_s\gamma$), and BR($K \to \pi^+\nu\bar{\nu}$), respectively. This emphasises the need for high-precision measurements of $b \to s/d$, but also of $s \to d$ transitions such as the rare kaon decay $K \to \pi\nu\bar{\nu}$. The second prediction is that the CKM phase is the only source of CP violation. This implies that any phase measurement as in $B \to \phi K_s$ or $\Delta M_{B_{(s/d)}}$ is not sensitive to new physics. This is an additional assumption because the breakings of the flavour group and the discrete CP symmetry are in principle not connected at all. For example there is also a renormalisation-group invariant extension of the MFV

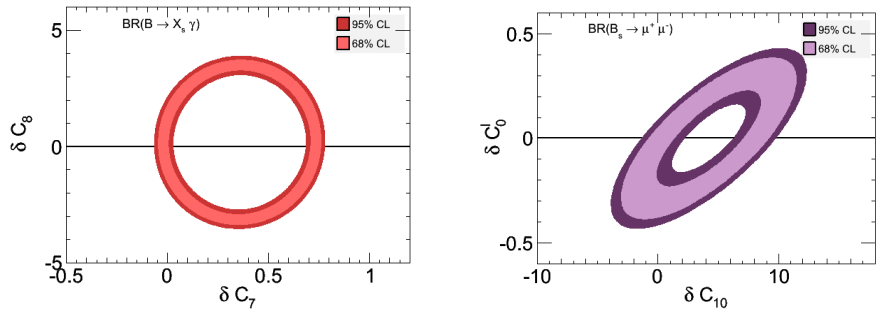

FIG. 21: 68% and 95% C.L. bounds on δC_7 and δC_8 induced by the inclusive decay $\bar{B} \to X_s\gamma$ (left) and on δC_{10} and δC_0^ℓ induced by the decay $B_s \to \mu^+\mu^-$ (right).

concept allowing for flavour-blind phases as was shown in Ref. [79]; however these lead to nontrivial CP effects, which get strongly constrained by flavour-diagonal observables such as electric dipole moments [79]. So within the model-independent effective field theory approach of MFV we keep the minimality condition regarding CP. But in specific models like MSSM the discussion of additional CP phases within the MFV framework makes sense and can also allow for a natural solution of the well-known supersymmetric CP problem, see for example Refs. [80, 81].

The application of the MFV hypothesis to the MSSM offers two attractive features. Most interestingly, the MFV hypothesis can serve as a substitute for R-parity in the MSSM [82, 83]. MFV is sufficient to forbid a too fast proton decay because when the MFV hypothesis is applied to R-parity violating terms, the spurion expansion leads to a suppression by neutrino masses and light-charged fermion masses, in this sense MFV within the MSSM can be regarded as a natural theory for R-parity violation. Secondly, the MFV framework is renormalisation-group invariant by construction, however, it is not clear that the hierarchy between the spurion terms is preserved when running down from the high scale to the low electroweak scale. Without this conservation of hierarchy, the MFV hypothesis would lose its practicability. However, as explicitly shown in Refs. [84, 85], a MFV-compatible change of the boundary conditions at the high scale has barely any influence on the low-scale spectrum.

It is worth mentioning that the MFV hypothesis solves the NP flavour problem only formally. One still has to find explicit dynamical structures to realise the MFV hypothesis like gauge-mediated supersymmetric theories. And of course the MFV hypothesis is not a theory of flavour; it does not explain the hierarchical structure of the CKM matrix and the large mass splittings of the SM fermions.

We stress that the MFV hypothesis is far from being verified. There is still room for sizeable new effects, and new flavour structures beyond the Yukawa couplings are still compatible with the present data because the flavour sector has been tested only at the 10% level especially in the $b \to s$ transitions.

Based on the recent LHCb data a new analysis of rare decays within the MFV effective theory was presented [86]. Here we update that analysis using the latest LHCb result for $\mathrm{BR}(B_s \to \mu^+\mu^-)$ and the new HFAG world average for $\mathrm{BR}(B \to X_s\gamma)$.

Within the MFV effective Hamiltonian one singles out only five relevant $b \to s$ operators (and also $b \to d$ operators with obvious replacements):

$$\begin{aligned}\mathcal{H}_{\rm eff}^{b\to s} &= -\frac{4G_F}{\sqrt{2}}[V_{us}^*V_{ub}(C_1^cP_1^u + C_2^cP_2^u) \\ &\quad + V_{cs}^*V_{cb}(C_1^cP_1^c + C_2^cP_2^c)] \\ &\quad - \frac{4G_F}{\sqrt{2}}\sum_{i=3}^{10}[(V_{us}^*V_{ub} + V_{cs}^*V_{cb})C_i^c \\ &\quad + V_{ts}^*V_{tb}C_i^t]P_i + V_{ts}^*V_{tb}C_0^\ell P_0^\ell \;+\; \text{h.c.}\end{aligned} \tag{20}$$

where the relevant operators are

$$\begin{aligned}P_7 &= \tfrac{e}{16\pi^2}m_b(\bar{s}_L\sigma^{\mu\nu}b_R)F_{\mu\nu}\,, \\ P_8 &= \tfrac{g_s}{16\pi^2}m_b(\bar{s}_L\sigma^{\mu\nu}T^ab_R)G^a_{\mu\nu}\,, \\ P_9 &= \tfrac{e^2}{16\pi^2}(\bar{s}_L\gamma_\mu b_L)\textstyle\sum_\ell(\bar{\ell}\gamma^\mu\ell)\,, \\ P_{10} &= \tfrac{e^2}{16\pi^2}(\bar{s}_L\gamma_\mu b_L)\textstyle\sum_\ell(\bar{\ell}\gamma^\mu\gamma_5\ell)\,, \\ P_0^\ell &= \tfrac{e^2}{16\pi^2}(\bar{s}_Lb_R)(\bar{\ell}_R\ell_L)\,.\end{aligned} \tag{21}$$

The NP contributions to the corresponding Wilson coefficients can be parametrised as:

$$\delta C_i = C_i^{\rm MFV} - C_i^{\rm SM}\,. \tag{22}$$

We scan over δC_7, δC_8, δC_9, δC_{10} and δC_0^ℓ in order to obtain constraints on the Wilson coefficients based on the experimental results. Consecutively, for each point, the flavour observables are computed with `SuperIso` [87, 88]. The obtained values are compared to the experimental results by calculating the χ^2 in the usual way and the global fits are obtained by minimisation of the χ^2.

The individual constraints from the new $\mathrm{BR}(\bar{B} \to X_s\gamma)$ and $\mathrm{BR}(B_s \to \mu^+\mu^-)$ results are displayed in Figure 21. As compared to the previous constraints in [86],

Observable	Experiment (post-LHCb)	Experiment (pre-LHCb)	SM prediction [88]
$\mathrm{BR}(B_s \to \mu^+\mu^-)$	$(3.2\ ^{+1.4}_{-1.2}\ ^{+0.5}_{-0.3}) \times 10^{-9}$ [44]	$< 5.8 \times 10^{-8}$ [89]	$(3.53 \pm 0.38) \times 10^{-9}$
$\langle dBR/dq^2(B \to K^*\mu^+\mu^-)\rangle_{q^2\in[1,6]\mathrm{GeV}^2}$	$(0.42 \pm 0.04 \pm 0.04) \times 10^{-7}$ [90]	$(0.32 \pm 0.11 \pm 0.03) \times 10^{-7}$ [91]	$(0.47 \pm 0.27) \times 10^{-7}$
$\langle dBR/dq^2(B \to K^*\mu^+\mu^-)\rangle_{q^2\in[14.18,16]\mathrm{GeV}^2}$	$(0.59 \pm 0.07 \pm 0.04) \times 10^{-7}$ [90]	$(0.83 \pm 0.20 \pm 0.07) \times 10^{-7}$ [91]	$(0.71 \pm 0.18) \times 10^{-7}$
$\langle A_{FB}(B \to K^*\mu^+\mu^-)\rangle_{q^2\in[1,6]\mathrm{GeV}^2}$	$-0.18 \pm 0.06 \pm 0.02$ [90]	$0.43 \pm 0.36 \pm 0.06$ [91]	-0.06 ± 0.05
$\langle A_{FB}(B \to K^*\mu^+\mu^-)\rangle_{q^2\in[14.18,16]\mathrm{GeV}^2}$	$0.49 \pm 0.06 \pm 0.05$ [90]	$0.42 \pm 0.16 \pm 0.09$ [91]	0.44 ± 0.10
$q_0^2(A_{FB}(B \to K^*\mu^+\mu^-))$	$4.9^{+1.1}_{-1.3}\ \mathrm{GeV}^2$ [90]	–	$4.26 \pm 0.34\ \mathrm{GeV}^2$
$\langle F_L(B \to K^*\mu^+\mu^-)\rangle_{q^2\in[1,6]\mathrm{GeV}^2}$	$0.66 \pm 0.06 \pm 0.04$ [90]	$0.50 \pm 0.30 \pm 0.03$ [91]	0.72 ± 0.13
$\mathrm{BR}(B \to X_s\gamma)$	$(3.43 \pm 0.21 \pm 0.07) \times 10^{-4}$ [59]	$(3.43 \pm 0.21 \pm 0.07) \times 10^{-4}$ [59]	$(3.08 \pm 0.24) \times 10^{-4}$
$\Delta_0(B \to K^*\gamma)$	$(5.2 \pm 2.6) \times 10^{-2}$ [59]	$(5.2 \pm 2.6) \times 10^{-2}$ [59]	$(8.0 \pm 3.9) \times 10^{-2}$
$\mathrm{BR}(B \to X_d\gamma)$	$(1.41 \pm 0.57) \times 10^{-5}$ [92, 93]	$(1.41 \pm 0.57) \times 10^{-5}$ [92, 93]	$(1.49 \pm 0.30) \times 10^{-5}$
$\mathrm{BR}(B \to X_s\mu^+\mu^-)_{q^2\in[1,6]\mathrm{GeV}^2}$	$(1.60 \pm 0.68) \times 10^{-6}$ [63, 64]	$(1.60 \pm 0.68) \times 10^{-6}$ [63, 64]	$(1.78 \pm 0.16) \times 10^{-6}$
$\mathrm{BR}(B \to X_s\mu^+\mu^-)_{q^2>14.4\mathrm{GeV}^2}$	$(4.18 \pm 1.35) \times 10^{-7}$ [63, 64]	$(4.18 \pm 1.35) \times 10^{-7}$ [63, 64]	$(2.19 \pm 0.44) \times 10^{-7}$

TABLE I: Post- and pre-LHCb results for rare decays with the updated SM predictions.

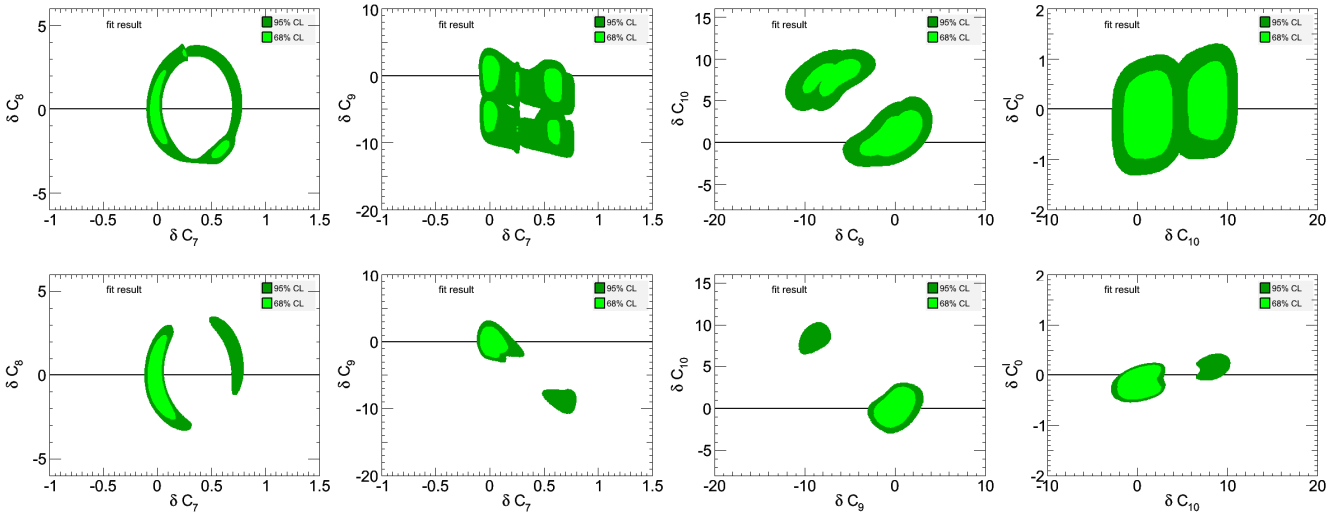

FIG. 22: Global MFV fit to the various NP coefficients δC_i in the MFV effective theory *without* (upper panel) and *with* experimental data of LHCb (lower panel).

the region favoured by $\mathrm{BR}(\bar{B} \to X_s\gamma)$ is only slightly shifted, and the constraints from the upper bound of $\mathrm{BR}(B_s \to \mu^+\mu^-)$ weakened while the lower bound now excludes the central region.

Two global MFV fits are given in Figure 22 to make the significance of the latest LHCb data manifest. In the first row, the experimental data before the start of the LHCb experiment are used (pre-LHCb), while the plots in the second row include the latest LHCb measurements (post-LHCb), as given in Table I. Here C_8 is mostly constrained by $\bar{B} \to X_{s,d}\gamma$, while C_7 is constrained by many other observables as well. C_9 is highly affected by $b \to s\mu^+\mu^-$ (inclusive and exclusive). C_{10} is in addition further constrained by $B_s \to \mu^+\mu^-$. The coefficient C_0^l of the scalar operator is dominantly constrained by $B_s \to \mu^+\mu^-$. There are always two allowed regions at 95% C.L. in the correlation plots within the post-LHCb fit; one corresponds to SM-like MFV coefficients and one to coefficients with flipped sign. The allowed region with the SM is more favoured. The various δC_i-correlation plots show the flipped-sign for C_7 is only possible if C_9 and C_{10} receive large non-standard contributions which finally also change the sign of these coefficients. With the help of the results of the global fit, which restricts the NP contributions δC_i, we can now derive several interesting predictions for observables which are not yet well measured. This analysis also allows to spot the observables which still allow for relatively large deviations from the SM (even in the MFV benchmark scenario). The following MFV predictions at the 95% C.L. are of particular interest:

$$1.0 \times 10^{-5} < \mathrm{BR}(\bar{B} \to X_d\gamma) < 4.0 \times 10^{-5}\,, \quad (23)$$

$$\mathrm{BR}(B_d \to \mu^+\mu^-) < 3.8 \times 10^{-10}. \quad (24)$$

The present experimental results are [44, 92, 93]:

$$\mathrm{BR}(\bar{B} \to X_d\gamma)_{\mathrm{Exp.}} = (1.41 \pm 0.57) \times 10^{-5}\,, \quad (25)$$

$$\mathrm{BR}(B_d \to \mu^+\mu^-)_{\mathrm{Exp.}} < 9.4 \times 10^{-10}. \quad (26)$$

So the present $\bar{B} \to X_d\gamma$ measurement is already below the MFV bound and is nicely consistent with the correlation between the decays $\bar{B} \to X_s\gamma$ and $\bar{B} \to X_d\gamma$ predicted in the MFV scenario. In the case of the leptonic decay $B_d \to \mu^+\mu^-$, however, the MFV bound is stronger than the current experimental limit. Moreover there are still sizeable deviations from the SM prediction possible within and also beyond the MFV bound but an enhancement by orders of magnitudes (*i.e.* due to large $\tan\beta$ effects) is already ruled out by the latest measurements. Clearly, a measurement of $B_d \to \mu^+\mu^-$ beyond the MFV bound would signal the existence of new flavour structures beyond the Yukawa couplings.

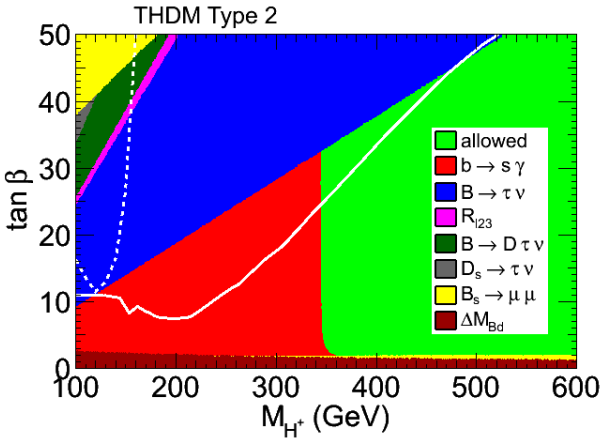

FIG. 23: Constraints from flavour observables in the THDM type II in the plane (m_{H^+},$\tan\beta$).

V. OUTLOOK AND FUTURE OPPORTUNITIES

Many efforts have been deployed in the past in order to calculate as precisely as possible the low energy observables from flavour physics. This global effort led to a very satisfying situation now as we have access to several observables for which the theoretical predictions have reached high levels of accuracy. The reliability of the results from flavour physics (as compared to the other indirect searches such as in the dark matter sector where strong astrophysical and cosmological assumptions are needed) makes the flavour observables the premier actors in the search for indirect NP effects. Rare B decays, and in particular $b \to s\gamma$ are the main assets here. Also, the fact that multiple observables are available offers the opportunity for important cross checks.

In addition, any discovery at a high p_T experiment must be consistent with the measurement from flavour experiments – the contrary would indicate an inconsistency in the theory. The role of flavour physics is therefore very important in the LHC era.

An example of the interplay between flavour constraints and LHC direct search results is displayed in Figure 23 for the THDM type II, where BR($b \to s\gamma$) excludes the charged Higgs mass below 345 GeV for any value of $\tan\beta$. BR($B \to \tau\nu$) on the other hand constrains more strongly larger values of $\tan\beta$. These constraints can be compared to the latest limit from the direct searches of the charged Higgs boson by ATLAS [94] (dashed white line), where flavour constraints are clearly stronger, or with the CMS limit from direct $H/A \to \tau^+\tau^-$ searches [95] (solid white line) where one notices the consistency and complementarity of the direct and indirect results. Another concrete example is the understanding of the newly discovered Higgs-like particle properties where imposing consistency with the $b \to s\gamma$ and $B_s \to \mu^+\mu^-$ results allows to discriminate between some of the underlying hypotheses.

We know that the stabilisation of the electroweak sector needs a nontrivial flavour structure which still has to be clearly identified. In spite of the fact that the first two years of high-statistics measurements of LHCb have not found any NP in FCNCs, still sizeable deviations from the MFV scenario are possible in various flavour observables. Thus, higher precision is needed to separate small deviations from the MFV benchmark.

Also in other future scenarios for particle physics, flavour physics will be important. For example, in case no NP is discovered next to one scalar Higgs particle, the flavour precision experiments may show us the way to the NP energy scale. FCNCs provide indirect information about scales which are not accessible by the direct search.

There are great experimental opportunities in flavour physics in the near future which will push the experimental precision to its limit. There are B physics programs at LHC at all three experiments at CERN. Especially LHCb will collect five times more data than the present data set. The copious production of all flavours of B mesons at the LHC, together with the unique particle-identification capabilities of the LHCb detector, makes it possible to investigate a wide range of decay channels that have not been accessible to previous experiments. Most of them have been discussed in this report like the CP-violating phase β_s, and searches of new physics effects via the rare decay modes $B \to K^*\mu\mu$ and $B_s \to \mu\mu$, but also the measurement of the unitarity angle γ and $B_s \to \phi\phi$. An upgrade of the LHCb experiment with a final integrated luminosity of 5 fb^{-1} to 50 fb^{-1} is planned and already approved [96].

There are also forthcoming experiments measuring rare K decays such as $K^+ \to \pi^+\nu\bar{\nu}$ and $K_L \to \pi^0\nu\bar{\nu}$ [97, 98] which are extremely sensitive to possible new degrees of freedom and are largely unexplored.

In addition, two Super-B factories, Belle II at KEK [99, 100] and SuperB in Italy [101–103], have been approved and partially funded to accumulate two orders of magnitude larger data samples. The Super-B factories are actually Super-*Flavour* factories (SFF): Besides precise B measurements - for example, the present experimental error of BR($B \to \tau\nu$) discussed above will be reduced

from 20% down to 4% improving the NP reach of this observable significantly – the SFF allow for precise analyses of CP violation in charm and of lepton flavour-violating modes like $\tau \to \mu\gamma$ (see Ref. [105]). The results will be highly complementary to those on several important observables related to B_s meson oscillations, kaon and muon decays that will be measured elsewhere.

Most important are the opportunities of a SFF for lepton flavour physics. The sensitivity for τ physics is far superior to any other existing or proposed experiment, and the physics reach can be extended even further by the possibility to operate with polarised beams. The study of the correlation of neutrino properties with flavour phenomena in the charged-lepton and in the quark sector, *e.g.* charged-lepton flavour violation, is also an important target. Pushing the present limits on $\mu \leftrightarrow e$ and $\mu \leftrightarrow \tau$ transitions might lead to important insight. The combined information on μ and τ flavour violating decays that will be provided by the MEG experiment [104] together with a SFF [105] may shed light on the mechanism responsible for lepton flavour violation.

Acknowledgement

TH thanks the organisers of PASCOS2012 for the great conference and for the kind hospitality. He also thanks the CERN theory group for its hospitality during his regular visits to CERN where part of this work was written

[1] BaBar Collaboration: `http://www.slac.stanford.edu/BFROOT`
[2] Belle Collaboration: `http://belle.kek.jp`
[3] CDF Collaboration: `http://www-cdf.fnal.gov/physics/new/bottom/bottom.html`
[4] D0 Collaboration: `http://www-d0.fnal.gov/Run2Physics/WWW/results/b.htm`
[5] LHCb Collaboration: `http://lhcb.web.cern.ch/lhcb/`
[6] M. Kobayashi and T. Maskawa, Prog. Theor. Phys. **49** (1973) 652.
[7] N. Cabibbo, Phys. Rev. Lett. **10** (1963) 531.
[8] CKMfitter Group (J. Charles et al.), Eur. Phys. J. C41, (2005) 1 [hep-ph/0406184], and updated results and plots available at: `http://ckmfitter.in2p3.fr`.
[9] ATLAS Collaboration: `http://atlas.web.cern.ch`
[10] CMS Collaboration: `http://cms.web.cern.ch`
[11] T. Hurth and M. Nakao, Ann. Rev. Nucl. Part. Sci. **60** (2010) 645 [arXiv:1005.1224 [hep-ph]].
[12] T. Hurth, Rev. Mod. Phys. **75** (2003) 1159 [hep-ph/0212304].
[13] F. Mahmoudi, arXiv:1205.3099 [hep-ph].
[14] T. Hurth and S. Kraml, AIP Conf. Proc. **1441** (2012) 713 [arXiv:1110.3804 [hep-ph]].
[15] L. Randall and R. Sundrum, Phys. Rev. Lett. **83** (1999) 3370 [hep-ph/9905221].
[16] Y. Grossman and M. Neubert, Phys. Lett. B **474** (2000) 361 [hep-ph/9912408].
[17] T. Gherghetta and A. Pomarol, Nucl. Phys. B **586** (2000) 141 [hep-ph/0003129].
[18] A. Lenz *et al.*, Phys. Rev. D **83** (2011) 036004 [arXiv:1008.1593 [hep-ph]].
[19] R. Aaij *et al.* [LHCb Collaboration], Phys. Rev. Lett. **108** (2012) 101803 [arXiv:1112.3183 [hep-ex]].
[20] R. Aaij *et al.* [LHCb Collaboration], Phys. Rev. Lett. **108** (2012) 241801 [arXiv:1202.4717 [hep-ex]].
[21] A. Lenz and U. Nierste, arXiv:1102.4274 [hep-ph].
[22] V. M. Abazov *et al.* [D0 Collaboration], Phys. Rev. D **84** (2011) 052007 [arXiv:1106.6308 [hep-ex]].
[23] A. Lenz, arXiv:1108.1218 [hep-ph].
[24] V. M. Abazov *et al.* [D0 Collaboration], arXiv:1207.1769 [hep-ex].
[25] LHCb Collaboration, LHCb-CONF-2012-022.
[26] A. Lenz *et al.*, Phys. Rev. D **86** (2012) 033008 [arXiv:1203.0238 [hep-ph]].
[27] U. Egede, T. Hurth, J. Matias, M. Ramon and W. Reece, JHEP **0811** (2008) 032 [arXiv:0807.2589 [hep-ph]].
[28] U. Egede, T. Hurth, J. Matias, M. Ramon and W. Reece, JHEP **1010** (2010) 056 [arXiv:1005.0571 [hep-ph]].
[29] F. Mahmoudi, S. Neshatpour and J. Orloff, JHEP **1208** (2012) 092 [arXiv:1205.1845 [hep-ph]].
[30] J. Matias, F. Mescia, M. Ramon and J. Virto, JHEP **1204** (2012) 104 [arXiv:1202.4266 [hep-ph]].
[31] C. Bobeth, G. Hiller and D. van Dyk, JHEP **1007** (2010) 098 [arXiv:1006.5013 [hep-ph]].
[32] W. Altmannshofer *et al.*, JHEP **0901** (2009) 019 [arXiv:0811.1214 [hep-ph]].
[33] C. Bobeth, G. Hiller and G. Piranishvili, JHEP **0807** (2008) 106 [arXiv:0805.2525 [hep-ph]].
[34] C. Bobeth, G. Hiller and D. van Dyk, JHEP **1107** (2011) 067 [arXiv:1105.0376 [hep-ph]].
[35] F. Beaujean, C. Bobeth, D. van Dyk and C. Wacker, JHEP **1208** (2012) 030 [arXiv:1205.1838 [hep-ph]].
[36] C. -S. Huang, W. Liao and Q. -S. Yan, Phys. Rev. D **59** (1999) 011701 [hep-ph/9803460].
[37] C. Hamzaoui, M. Pospelov and M. Toharia, Phys. Rev. D **59** (1999) 095005 [hep-ph/9807350].
[38] K. S. Babu and C. F. Kolda, Phys. Rev. Lett. **84** (2000) 228 [hep-ph/9909476].
[39] R. Aaij *et al.* [LHCb Collaboration], Phys. Rev. Lett. **108** (2012) 231801 [arXiv:1203.4493 [hep-ex]].
[40] S. Chatrchyan *et al.* [CMS Collaboration], JHEP **1204** (2012) 033 [arXiv:1203.3976 [hep-ex]].
[41] T. Aaltonen *et al.* [CDF Collaboration], Phys. Rev. Lett. **107** (2011) 191801 [arXiv:1107.2304 [hep-ex]].
[42] G. Aad *et al.* [ATLAS Collaboration], Phys. Lett. B **713** (2012) 387 [arXiv:1204.0735 [hep-ex]].
[43] LHCb/CMS/ATLAS Collaborations: LHCb-CONF-2012-017,CMS PAS BPH-12-009,ATLAS-COM-CONF-2012-090.
[44] R. Aaij *et al.* [LHCb Collaboration], arXiv:1211.2674 [hep-ex].

[45] P. Dimopoulos *et al.* [ETM Collaboration], JHEP **1201** (2012) 046 [arXiv:1107.1441].

[46] A. Bazavov *et al.* [Fermilab Latt./MILC Collab.], Phys. Rev. D **85** (2012) 114506 [arXiv:1112.3051 [hep-lat]].

[47] E. T. Neil *et al.* [Fermilab Latt./MILC Collab.], PoS LATTICE **2011** (2011) 320 [arXiv:1112.3978 [hep-lat]].

[48] H. Na *et al.*, Phys. Rev. D **86** (2012) 034506 [arXiv:1202.4914 [hep-lat]].

[49] C. McNeile *et al.*, Phys. Rev. D **85** (2012) 031503 [arXiv:1110.4510].

[50] C. Davies, PoS LATTICE **2011** (2011) 019 [arXiv:1203.3862 [hep-lat]].

[51] K. De Bruyn *et al.*, Phys. Rev. D **86** (2012) 014027 [arXiv:1204.1735 [hep-ph]].

[52] K. De Bruyn *et al.*, Phys. Rev. Lett. **109** (2012) 041801 [arXiv:1204.1737 [hep-ph]].

[53] A. J. Buras, J. Girrbach, D. Guadagnoli and G. Isidori, arXiv:1208.0934 [hep-ph].

[54] A. G. Akeroyd, F. Mahmoudi and D. Martinez Santos, JHEP **1112** (2011) 088 [arXiv:1108.3018 [hep-ph]].

[55] S. Chatrchyan *et al.* [CMS Collaboration], Phys. Rev. Lett. **107**, 221804 (2011).

[56] CMS Collaboration, CMS-PAS-SUS-12-005.

[57] M. Benzke, S. J. Lee, M. Neubert and G. Paz, JHEP **1008**, 099 (2010) [arXiv:1003.5012 [hep-ph]].

[58] M. Misiak *et al.*, Phys. Rev. Lett. **98**, 022002 (2007) [arXiv:hep-ph/0609232].

[59] Y. Amhis *et al.* [Heavy Flavor Averaging Group Collaboration], arXiv:1207.1158 [hep-ex] and online updates at `http://www.slac.stanford.edu/xorg/hfag`

[60] C. Greub *et al.*, Nucl. Phys. B **853** (2011) 240 [arXiv:1105.1330 [hep-ph]].

[61] C. Greub, T. Hurth, V. Pilipp and C. Schuepbach, arXiv:1111.3692 [hep-ph].

[62] T. Huber, T. Hurth and E. Lunghi, Nucl. Phys. B **802** (2008) 40 [arXiv:0712.3009 [hep-ph]].

[63] B. Aubert *et al.* [BABAR Collaboration], Phys. Rev. Lett. **93** (2004) 081802 [hep-ex/0404006].

[64] M. Iwasaki *et al.* [Belle Collaboration], Phys. Rev. D **72** (2005) 092005 [hep-ex/0503044].

[65] T. Hurth, AIP Conf. Proc. **1441** (2012) 678 [arXiv:1111.2367 [hep-ph]].

[66] J. P. Lees *et al.* [BaBar Collaboration], Phys. Rev. Lett. **109** (2012) 101802 [arXiv:1205.5442 [hep-ex]].

[67] S. Fajfer, J. F. Kamenik and I. Nisandzic, Phys. Rev. D **85** (2012) 094025 [arXiv:1203.2654 [hep-ph]].

[68] D. Becirevic, N. Kosnik and A. Tayduganov, Phys. Lett. B **716** (2012) 208 [arXiv:1206.4977 [hep-ph]].

[69] J. A. Bailey *et al.*, Phys. Rev. Lett. **109** (2012) 071802 [arXiv:1206.4992 [hep-ph]].

[70] A. Crivellin, C. Greub and A. Kokulu, Phys. Rev. D **86** (2012) 054014 [arXiv:1206.2634 [hep-ph]].

[71] S. Fajfer, J. F. Kamenik, I. Nisandzic and J. Zupan, arXiv:1206.1872 [hep-ph].

[72] R. S. Chivukula and H. Georgi, Phys. Lett. B **188** (1987) 99.

[73] L. J. Hall and L. Randall, Phys. Rev. Lett. **65**, 2939 (1990).

[74] G. D'Ambrosio, G. F. Giudice, G. Isidori and A. Strumia, Nucl. Phys. B **645** (2002) 155 [hep-ph/0207036].

[75] T. Hurth, G. Isidori, J. F. Kamenik and F. Mescia, Nucl. Phys. B **808** (2009) 326 [arXiv:0807.5039 [hep-ph]].

[76] G. Isidori and D. M. Straub, Eur. Phys. J. C **72** (2012) 2103 [arXiv:1202.0464 [hep-ph]].

[77] W. Altmannshofer and D. M. Straub, JHEP **1208** (2012) 121 [arXiv:1206.0273 [hep-ph]].

[78] S. Descotes-Genon, D. Ghosh, J. Matias and M. Ramon, JHEP **1106** (2011) 099 [arXiv:1104.3342 [hep-ph]].

[79] T. Hurth, E. Lunghi and W. Porod, Nucl. Phys. B **704** (2005) 56 [arXiv:hep-ph/0312260].

[80] L. Mercolli and C. Smith, Nucl. Phys. B **817** (2009) 1 [arXiv:0902.1949 [hep-ph]].

[81] P. Paradisi and D. M. Straub, Phys. Lett. B **684** (2010) 147 [arXiv:0906.4551 [hep-ph]].

[82] E. Nikolidakis and C. Smith, Phys. Rev. D **77** (2008) 015021 [arXiv:0710.3129 [hep-ph]].

[83] C. Csaki, Y. Grossman and B. Heidenreich, Phys. Rev. D **85**, 095009 (2012) [arXiv:1111.1239 [hep-ph]].

[84] P. Paradisi, M. Ratz, R. Schieren and C. Simonetto, Phys. Lett. B **668** (2008) 202 [arXiv:0805.3989 [hep-ph]].

[85] G. Colangelo, E. Nikolidakis and C. Smith, Eur. Phys. J. C **59** (2009) 75 [arXiv:0807.0801 [hep-ph]].

[86] T. Hurth and F. Mahmoudi, Nucl. Phys. B **865** (2012) 461 [arXiv:1207.0688 [hep-ph]].

[87] F. Mahmoudi, Comput. Phys. Commun. **178** (2008) 745 [arXiv:0710.2067];

[88] Comput. Phys. Commun. **180** (2009) 1579 [arXiv:0808.3144].

[89] T. Aaltonen *et al.* [CDF Collaboration], Phys. Rev. Lett. **100** (2008) 101802 [arXiv:0712.1708 [hep-ex]].

[90] LHCb Collaboration, LHCb-CONF-2012-008.

[91] CDF Collaboration, CDF note 10047.

[92] P. del Amo Sanchez *et al.* [BABAR Collaboration], Phys. Rev. D **82** (2010) 051101 [arXiv:1005.4087 [hep-ex]].

[93] W. Wang, arXiv:1102.1925 [hep-ex].

[94] G. Aad *et al.* [ATLAS Collaboration], JHEP **1206** (2012) 039 [arXiv:1204.2760 [hep-ex]].

[95] S. Chatrchyan *et al.* [CMS Collaboration], Phys. Lett. B **713** (2012) 68 [arXiv:1202.4083 [hep-ex]].

[96] M. Merk [LHCb Collaboration], PoS BEAUTY **2011** (2011) 039.

[97] NA48 Collaboration: `http://na48.web.cern.ch/NA48/NA48-3`

[98] JPARC Kaon Collaboration: `http://kaon.kek.jp/~kpwg`

[99] T. Aushev *et al.*, arXiv:1002.5012 [hep-ex].

[100] T. Abe *et al.* [Belle II Collaboration], arXiv:1011.0352 [physics.ins-det].

[101] B. O'Leary *et al.* [SuperB Collaboration], arXiv:1008.1541 [hep-ex].

[102] D. G. Hitlin *et al.*, arXiv:0810.1312 [hep-ph].

[103] M. Bona *et al.* [SuperB Collaboration], arXiv:0709.0451 [hep-ex].

[104] MEG Collaboration: `http://meg.web.psi.ch`

[105] T. Browder, M. Ciuchini, T. Gershon, M. Hazumi, T. Hurth, Y. Okada and A. Stocchi, JHEP **0802** (2008) 110 [arXiv:0710.3799 [hep-ph]].